PUBLICATION 4

Impedance and quality factor of mutually coupled multiport antennas

In: Microwave and Optical Technology Letters 2008.
Vol. 50, No. 8, pp. 2034–2039.

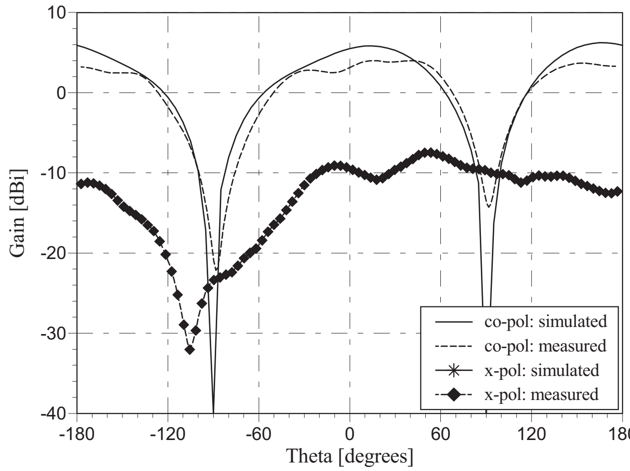

Figure 8 Simulated and measured E-plane radiation patterns at 5.2 GHz for the dual-band CPW-fed slot antenna [$\varphi = 180°$, with reference to Fig. 1(a)]

and 8. The maximum simulated gain of the antenna was found to be ~6 dBi in both the lower and upper frequency bands, and the measured gain was slightly lower. The irregularities in the E-plane measured results around $\theta = 90°$ for both the co- and cross-polarization patterns are because of the feed cable, which was connected in the measurement plane.

4. CONCLUSIONS

In this article, a simple impedance matching design approach to obtain dual-band performance from a single CPW-fed slot was described. Although the upper and lower bandwidths were only 8 and 6%, respectively, the antenna is ideal for dual-band WLAN applications in the 2.4 and 5.2 GHz bands. The same design approach can also be followed to design dual-band antennas with different f_2/f_1 ratios. The two elements (slot and terminated stub) forming the antenna can be designed separately and then combined—final tuning of the stub parameters can then be done to satisfy the design requirements. The radiation patterns at both the upper and lower band were well-formed, had similar gain in both frequency bands, and good cross-polarization characteristics.

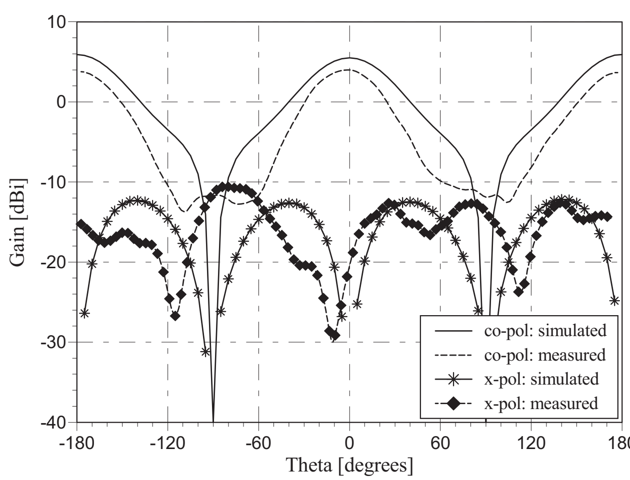

Figure 9 Simulated and measured H-plane radiation patterns at 5.2 GHz for the dual-band CPW-fed slot antenna [$\varphi = 90°$, with reference to Fig. 1(a)]

REFERENCES

1. M.-H. Ho and G.-L. Chen, Reconfigured slot-ring antenna for 2.4/5.2 GHz dual-band operations, IET Microwave Antennas Propag 1 (2007), 712–717.
2. A.A. Omar, M.C. Scardelletti, Z.M. Hejazi, and N. Dib, Design and measurement of self-matched dual-frequency coplanar waveguide-fed-slot antennas, IEEE Trans Antennas Propag AP-55 (2007), 223–226.
3. D. Llorens, P. Otero, and C. Camacho-Penalosa, Dual-band, single CPW port, planar-slot antenna, IEEE Trans Antennas Propag AP-51 (2003), 137–139.
4. Y.-C. Lin and K.-J. Hung, Design of dual-band slot antenna with double T-match stubs, Electron Lett 42 (2006), 438–439.
5. Y.-C. Chen, S.-Y. Chen, and P. Hsu, Dual-band slot dipole antenna fed by a coplanar waveguide, IEEE AP-S Dig, Albuquerque, NM (2006), 3589–3592.
6. M.C. Mukandatimana, T.A. Denidni, and L. Talbi, Design of a new dual-band CPW-fed slot antenna for ISM applications, IEEE AP-S Dig, Monterey, CA (2004), 6–9.
7. Zeland Software, IE3D User's Manual, Release 12.1 (2007).

IMPEDANCE AND QUALITY FACTOR OF MUTUALLY COUPLED MULTIPORT ANTENNAS

Johan C.-E. Sten and Mervi Hirvonen
VTT Technical Research Centre of Finland, P.O. Box 1000, 02044 VTT Finland; Corresponding author: johan.sten@vtt.fi

Received 10 December 2007

ABSTRACT: *In this study, expressions for the radiation quality factor Q and the input impedance seen at any terminal of a multiport antenna are derived. It is shown computationally that because of the possibility to adjust the antenna current distribution through suitable feeding/loading a multiport antenna can perform lower Qs than a similar single-port antenna.* © 2008 Wiley Periodicals, Inc. Microwave Opt Technol Lett 50: 2034–2039, 2008; Published online in Wiley InterScience (www.interscience.wiley.com). DOI 10.1002/mop.23564

Key words: *multiport antenna; quality factor; mutual coupling; impedance matrix; input impedance*

1. INTRODUCTION

With the exception of large arrays, antennas are traditionally conceived as single-port devices. This is because mutual coupling, which is often very strong in small and compact antennas, is regarded as an unwanted nonideality to be eliminated or compensated to achieve a desired radiation characteristic [1]. In this article, a different viewpoint is taken, namely to look for the advantages of the mutual coupling for improving the antenna performance, in particular the radiation quality factor Q, which is an important design parameter for small antennas.

Previously, the Q of antennas with multiple ports have been studied in the case of totally isolated ports, which was observed to lead to an increasing Q [2]. However, in [2], only the energy involved in the reactive part of the spherical multipole fields was taken into account, whereas the interior stored energy due to the fields inside the smallest sphere that can be drawn around the antenna was assumed to be zero. Our case is more realistic as it takes into consideration the total stored energy and the mutual coupling. In this article, we show by means of computational examples that by providing an antenna—in our case a short wire antenna near a ground plane—with several mutually coupled input/output ports and choosing their feed point amplitudes suitably, a lower Q (and, implicitly, a potentially broader bandwidth) can actually be achieved than by feeding only one port at a time. Furthermore, we compare the tuning using a single reactive element at the feed point with tuning by means of a set of distributed reactive load impedances embedded inside the antenna. For this purpose, a formula for the input impedance viewed from one of the ports of a general N-port antenna is derived and given in the Appendix.

As a preliminary, we first establish the circuit equations governing the antenna system modeled as a lossy linear network [3]. Enumerating the input/output ports of the N-port antenna $i = 1, 2, \ldots, N$, the current intensities I_i and the voltages V_i at the ports (the dimensions of which are assumed to be sufficiently small in terms of the wavelength) are interrelated by Kirchhoff's network equations, which can be condensed as an $N \times N$ impedance matrix (see, e.g., [3, 4]) viz,

$$\begin{pmatrix} V_1 \\ V_2 \\ \vdots \\ V_N \end{pmatrix} = \begin{pmatrix} z_{11} & z_{12} & \cdots & z_{1N} \\ z_{21} & \ddots & & z_{2N} \\ \vdots & & \ddots & \\ z_{N1} & \cdots & & z_{NN} \end{pmatrix} \begin{pmatrix} I_1 \\ I_2 \\ \vdots \\ I_N \end{pmatrix} \tag{1}$$

abbreviated $\bar{V} = \bar{\bar{Z}}\bar{I}$ (or equivalently $\bar{I} = \bar{\bar{Y}}\bar{V}$ in terms of the admittance matrix $\bar{\bar{Y}} = \bar{\bar{Z}}^{-1}$).

The concomitant scattering matrix $\bar{\bar{S}}$ describing the interaction of the antenna with external sources and load impedances is defined by means of the incoming and the reflected wave vectors, $\bar{w}^+$ and $\bar{w}^-$, respectively, as

$$\bar{w}^+ = \bar{V} + \bar{\bar{Z}}_L\bar{I} \quad \text{and } \bar{w}^- = \bar{V} - \bar{\bar{Z}}_L\bar{I} \tag{2}$$

where $\bar{\bar{Z}}_L$ signifies an $N \times N$ diagonal matrix having as its diagonal entries the load-impedances $z_{L1}, z_{L2}, \ldots, z_{LN}$ connected to the respective terminal. Combining (1) and (2) yields

$$\bar{w}^- = (\bar{\bar{Z}} - \bar{\bar{Z}}_L)(\bar{\bar{Z}}_L + \bar{\bar{Z}})^{-1}\bar{w}^+ \tag{3}$$

$$\text{where } \bar{\bar{S}} = (\bar{\bar{Z}} - \bar{\bar{Z}}_L)(\bar{\bar{Z}}_L + \bar{\bar{Z}})^{-1}.$$

2. ANTENNA QUALITY FACTOR

It is a well-known fact that the bandwidth of a resonant device (such as an antenna) is closely related to the quality factor Q [5–8]. The Q is generally defined as 2π times the ratio of the energy stored by the device per cycle and the energy lost during the same time interval, i.e.,

$$Q = \omega \frac{W^{\mathrm{E,stored}} + W^{\mathrm{M,stored}}}{P^{\mathrm{loss}}} \tag{4}$$

where $W^{\mathrm{E,stored}}$ and $W^{\mathrm{M,stored}}$ are, respectively, the time average electric and magnetic energy stored, and P^{loss} is the average dissipated power, which is equal to the power radiated P^{rad} when the antenna is lossless, as will be the case in the following.

However, when applying this definition to antennas, a problem arises as follows: as the electromagnetic energy of an antenna is dispersed all around the surrounding space, it is not immediately clear how the stored energy should be defined and measured. In particular, since a part of the energy is associated with the propagating fields, it is evident that this part of the energy should be extracted from the total energy. Because energy as a global quantity can be only indirectly estimated, we must find a way to relate it to the response of the device to the excitation by a time-harmonic signal (through the complex voltages and currents at the input/output ports).

To tackle the problem, we start from the identity (which Papas [9] termed as the "energy theorem")

$$\nabla \cdot \left(\frac{\partial \mathbf{E}}{\partial \omega} \times \mathbf{H}^* - \frac{\partial \mathbf{H}}{\partial \omega} \times \mathbf{E}^* \right) = -j\left[\frac{\partial(\omega\varepsilon)}{\partial \omega}\mathbf{E}\cdot\mathbf{E}^* + \frac{\partial(\omega\mu)}{\partial \omega}\mathbf{H}\cdot\mathbf{H}^* \right] - \frac{\partial \mathbf{E}}{\partial \omega}\cdot\mathbf{J}^* - \mathbf{E}^*\cdot\frac{\partial \mathbf{J}}{\partial \omega} \tag{5}$$

derivable from the time harmonic Maxwell equations by ω-differentiation [7, 9]. In deriving (5), a time dependence of $e^{j\omega t}$ has been assumed, since this will lead to a circuit description where positive reactances are interpreted as inductive and negative reactances as capacitive (the standard engineering convention). In the sequel, the last two terms involving conduction currents ($\mathbf{J}$) will be ignored as our primary interest at this point is the ideal case without (significant) losses. For a treatment of the more general case involving losses and material dispersion, we refer to [7, 10].

Let us next apply the theorem to a volume ν bounded from the inside by the antenna occupying the volume ν_0 and from the outside by a sphere $\nu_{r\to\infty}$, whose radius goes to infinity. Application of Gauss' divergence theorem gives

$$\int_{\partial\nu} \left(\frac{\partial \mathbf{E}}{\partial \omega} \times \mathbf{H}^* - \frac{\partial \mathbf{H}}{\partial \omega} \times \mathbf{E}^* \right)\cdot dS = -4j\left[\int_{\nu} \frac{1}{4}\frac{\partial(\omega\varepsilon)}{\partial \omega}\left|\mathbf{E}\right|^2 d\nu + \int_{\nu} \frac{1}{4}\frac{\partial(\omega\mu)}{\partial \omega}\left|\mathbf{H}\right|^2 d\nu \right], \tag{6}$$

where dS is a differential surface element and $\partial\nu$ is the bounding surface of the considered volume ν. The two volume integrals can be interpreted as generalizations (for dispersive materials) of the familiar energy integrals

$$W^{\mathrm{E}} = \int_{\nu} \frac{\varepsilon}{4}|\mathbf{E}(\mathbf{r})|^2 d\nu, \tag{7}$$

$$W^{\mathrm{M}} = \int_{\nu} \frac{\mu}{4}|\mathbf{H}(\mathbf{r})|^2 d\nu, \tag{8}$$

into which they reduce in the case that the medium is not dispersive ($\partial\varepsilon/\partial\omega = 0$ and $\partial\mu/\partial\omega = 0$). On the surface of the antenna $\partial\nu_0$, which we assume to be a perfectly conducting boundary, the integral vanishes everywhere except for the terminals, where it yields

$$\int_{\partial\nu_0} \left(\frac{\partial \mathbf{E}}{\partial \omega} \times \mathbf{H}^* - \frac{\partial H}{\partial \omega} \times \mathbf{E}^* \right)\cdot dS = -\sum_{i=1}^{N}\left(\frac{\partial V_i}{\partial \omega}I_i^* + \frac{\partial I_i}{\partial \omega}V_i^* \right) = -\frac{\partial \bar{V}^T}{\partial \omega}\bar{I}^* - \frac{\partial \bar{I}^T}{\partial \omega}\bar{V}^* \tag{9}$$

whereas on the radiation surface $\partial \nu_{r \to \infty}$, the integrand can be developed by using the long distance asymptotic expressions for the field vectors, viz,

$$\mathbf{E}(\mathbf{r}) \underset{r\to\infty}{\to} \mathbf{E}_\infty(\mathbf{u}_r)\frac{\exp(-jkr)}{r} \tag{10}$$

for the electric field, where $k = \omega\sqrt{\mu_0\varepsilon_0}$ and

$$\mathbf{E}_\infty(\mathbf{u}_r) = \lim_{r\to\infty}\frac{rE(r)}{\exp(-jkr)} \tag{11}$$

An exactly similar asymptotic relation applies to the magnetic field $\mathbf{H}(\mathbf{r})$. Thus, at $\partial \nu_{r\to\infty}$

$$\int_{\partial V_{r\to\infty}} \left(\frac{\partial \mathbf{E}}{\partial\omega}\times\mathbf{H}^* - \frac{\partial \mathbf{H}}{\partial\omega}\times\mathbf{E}^*\right)\cdot dS = \int_{\partial V_{r\to\infty}} \left(\frac{\partial \mathbf{E}_\infty}{\partial\omega}\times\mathbf{H}_\infty^* - \frac{\partial \mathbf{H}_\infty}{\partial\omega}\times E_\infty^* - 2jr\sqrt{\mu_0\varepsilon_0}\Re\{\mathbf{E}_\infty\times\mathbf{H}_\infty^*\}\right)\cdot\frac{dS}{r^2} \tag{12}$$

Identifying the radiated power with the expression

$$P^{\mathrm{rad}} = \int_{\partial V_{r\to\infty}} \frac{1}{2}\Re\{\mathbf{E}\times\mathbf{H}^*\}\cdot dS \tag{13}$$

and using $u_r \times \mathbf{E}\infty(\mathbf{u}_r) = \sqrt{\mu_0/\varepsilon_\infty}\mathbf{H}_\infty(u_r)$ and $\mathbf{u}_r\cdot\mathbf{E}\infty(\mathbf{u}_r) = 0$ the "energy theorem" (5) yields

$$\frac{\partial\bar{V}^T}{\partial\omega}\bar{I}^* + \frac{\partial\bar{I}^T}{\partial\omega}\bar{V}^* = 2\sqrt{\frac{\varepsilon_0}{\mu_0}}\int_{4\pi}\frac{\partial\mathbf{E}_\infty}{\partial\omega}\cdot\mathbf{E}_\infty^* d\Omega + 4j(W^{\mathrm{E}} + W^{\mathrm{M}} - r\sqrt{\mu_0\varepsilon_0}P^{\mathrm{rad}}) \tag{14}$$

denoting $d\Omega = \sin\theta d\theta d\varphi$. . The last term in the expression can be seen to involve three quantities having the quality of energy; W^{E}, W^{M}, and $r\sqrt{\mu_0\varepsilon_0}P^{\mathrm{rad}}$, each of which grow separately without a bound as $r\to\infty$. However, it can be shown that the quantities are interrelated and that the whole expression remains finite.

Let a be the radius of the smallest sphere that circumscribes the antenna. The total electromagnetic energy of the propagating field confined between the two concentric spheres of radii a and r must obviously be

$$W^{\mathrm{E,rad}} + W^{\mathrm{M,rad}} = \frac{(r-a)}{c_0}P^{\mathrm{rad}} \tag{15}$$

where $c_0 = \sqrt{\mu_0\varepsilon_0}$ is the speed of light. Within the sphere of radius a (the "antenna region") the energy is to be taken as completely stored, because the field in this region has strictly not been launched off the antenna, and thus it can in principle be decomposed in spherical waves propagating inward and outward. There is also some stored energy outside the sphere, which stems from the reactive part of the spherical multipole fields. Thus, in general, the total electromagnetic energy consists of a stored part and a radiated part, viz.,

$$W^{\mathrm{E}} + W^{\mathrm{M}} = W^{\mathrm{E,stored}} + W^{\mathrm{M,stored}} + \frac{(r-a)}{c_0}P^{\mathrm{rad}} \tag{16}$$

Invoking this relationship in (14) yields an expression for the requested quantity $W^{\mathrm{E,stored}} + W^{\mathrm{M,stored}}$, which inserted in (4) gives the result

$$Q = \frac{\omega}{4P^{\mathrm{rad}}}\Im\left\{\frac{\partial\bar{V}^T}{\partial\omega}\bar{I}^* + \frac{\partial\bar{I}^T}{\partial\omega}\bar{V}^*\right\} - \frac{\omega}{2P^{\mathrm{rad}}}\sqrt{\frac{\varepsilon_0}{\mu_0}}\Im\left\{\int_{4\pi}\frac{\partial\mathbf{E}_\infty}{\partial\omega}\cdot\mathbf{E}_\infty^* d\Omega\right\} + ka \tag{17}$$

In practice, either the voltages or the currents at the terminals are kept constant and independent of ω (meaning that either $\partial V_i/\partial\omega$ or $\partial I_i/\partial\omega$ vanish for every i and for all considered frequencies). Whichever condition one chooses, the same condition must also apply when the relevant field integral is computed from the fields. For instance, if $\partial I_i/\partial\omega = 0$ for all frequencies,

$$Q = \frac{\omega}{4P^{\mathrm{rad}}}\Im\left\{\sum_{i=1}^{N}\frac{\partial V_i}{\partial\omega}I_i^*\right\} - \frac{\omega}{2P^{\mathrm{rad}}}\sqrt{\frac{\varepsilon_0}{\mu_0}}\Im\left\{\int_{4\pi}\frac{\partial E_\infty}{\partial\omega}\cdot\mathbf{E}_\infty^* d\Omega\right\}_{\partial I_i/\partial\omega=0} + ka \tag{18}$$

$$P^{\mathrm{rad}} = \frac{1}{2}\Im\{\sum_{i=1}^{N}V_iI_i^*\} \tag{19}$$

In the case of a single feed point, (18) and (19) reduce to the classical formula in terms of the radiation resistance R^{rad} and reactance X [5, 6]

$$Q \approx \frac{\omega}{2R^{rad}}\frac{\partial X}{\partial\omega} \tag{20}$$

when the frequency dispersion of the far-field radiation [the integral quantity in (18)] is not evaluated due to its negligible (or zero) influence on the Q of small antennas [5]. The term ka has been dropped as well, as it is in most circumstances practically insignificant.

3. APPLICATIONS

As an application, we next present a number of simple computational examples to illustrate the use of multiple ports in connection with antennas that are small in terms of wavelength.

3.1. Optimizing Q Using Distributed Sources

First, let us consider the case of multiple feeds at different locations. For a given geometrical distribution of feed points, our aim is to find the combination of excitation current amplitudes that gives the best (lowest) antenna Q. As is well-known, the location of the feed point affects the current distribution on the antenna and the resulting radiation field pattern. In fact, even for negligible changes in the radiation pattern, the reactive near field and power may change significantly [11]. Thus, one can also expect to find clear differences between the cases in terms of antenna Q.

The antenna considered is a lossless horizontal wire tangential to a perfectly conducting ground plane. The ports are oriented horizontally and distributed evenly along the wire (see Fig. 1). The antenna Q-factor may now be calculated numerically using (18)

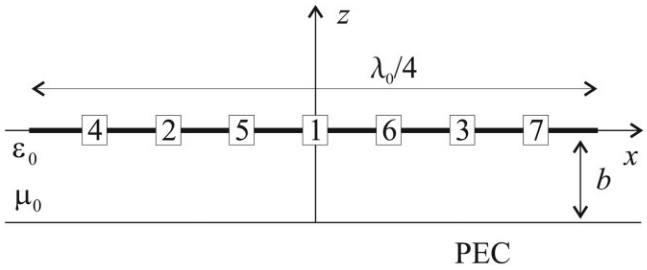

Figure 1 Horizontal dipole with multiple feed ports

and the simulated Z-matrix data by computing the port voltages V_i from the impressed excitation currents I_i. In the calculations, the second term (the far-field dispersion integral) in (18) has been neglected, since (as already mentioned) the field variations as a function ω are negligible in the case of radiation of low frequencies. In the field simulations (using HFSS by Ansoft Corp.), at the lowest considered frequency f_0 the wire has the length of $\lambda_0/4$ and the width of $0.0035\lambda_0$. The distance to the ground plane is $k_0 b = 0.1$.

In Figure 2, the Q-factors of the 1-port and 3-port cases are illustrated. In the 1-port case, the feed current $I_0 = 1$. In the 3-port case, the feed currents leading to minimum and maximum Q are sought numerically with a Matlab routine by letting the currents I_2 and I_3, which are assumed equal, to vary between 0 to 1, while keeping $I_0 = 1$. As can be seen from Figure 2, with a certain 3-port excitation of the wire, a remarkably lower Q when compared with the 1-port case can be achieved especially at lower frequencies (where the antenna is notably below resonance length). Near resonance $f/f_0 \approx 1.9$, however, the difference becomes less marked. The excitation currents leading to minimum and maximum Q values are shown in Figure 3. Evidently, the best result is obtained when the currents I_2 and I_3, appropriately weighted, reinforce the current I_1 at the middle, whereas the worst case is when $I_2 = I_3$ are both forced to zero (meaning that the antenna is made effectively shorter than its actual length). However, the Qs would be even larger if I_2 and I_3 were allowed to receive values more freely, that is, outside the range [0, 1] now considered. In Figure 3, one also notices that the values of I_2, I_3 giving optimal Q

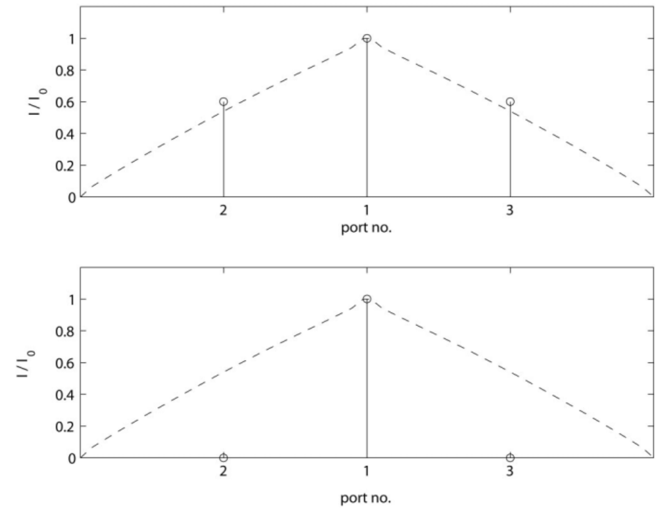

Figure 3 Excitation currents leading to minimum (top) and maximum (bottom) Q values, corresponding to Figure 2. For comparison, the current distribution along the wire in the 1-port case is depicted with a dashed line

differ only slightly from the strength of the current at the respective location of a centre-fed 1-port antenna.

Similarly, a 7-port case was calculated. The Q and the excitation currents corresponding to minimum and maximum Q-values are shown in Figures 4 and 5. As can be seen by comparing Figure 4 with Figure 2, by appropriate excitation of a 7-port antenna Q-factors slightly lower can be achieved than what is possible with a similar 3-port antenna.

3.2. *Optimizing Q Using Distributed Reactive Loads*

Next, let us search for the optimum (minimum) antenna Q by loading a 1-port, 3-port, and 7-port antenna, respectively, with appropriate reactive elements. In every case, the antenna structure is the same except for the varying number of ports.

Again, the antenna considered is a horizontal wire-dipole above a perfectly conducting ground plane. It is assumed to be fed horizontally at the mid-point, whereas the other ports are imposed vertically between the wire and the corresponding point on the ground plane below (see Fig. 6). For convenience, the structure is

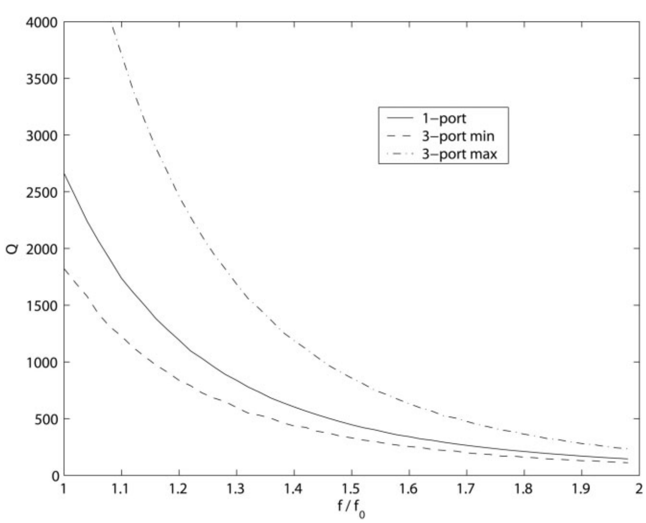

Figure 2 Minimum and maximum Q values obtained with excitation of three ports, assuming $I_2 = I_3 \in [0, 1]$

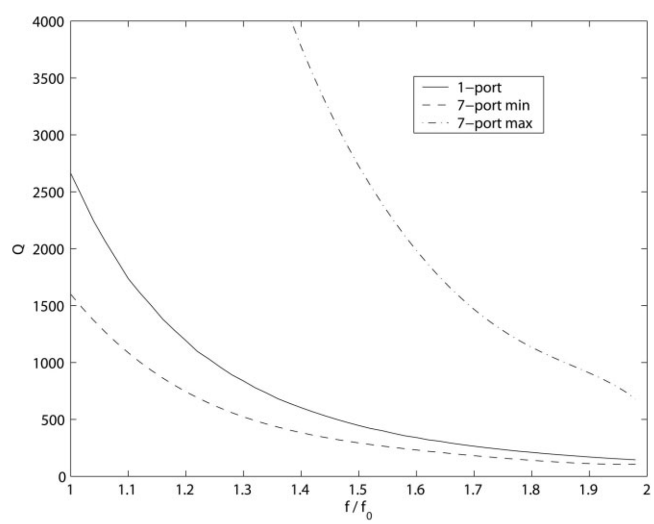

Figure 4 Minimum and maximum Q values obtained with 7-port excitation, assuming $I_2 = I_3$, $I_4 = I_7$, and $I_5 = I_6$ to vary in the range [0, 1]

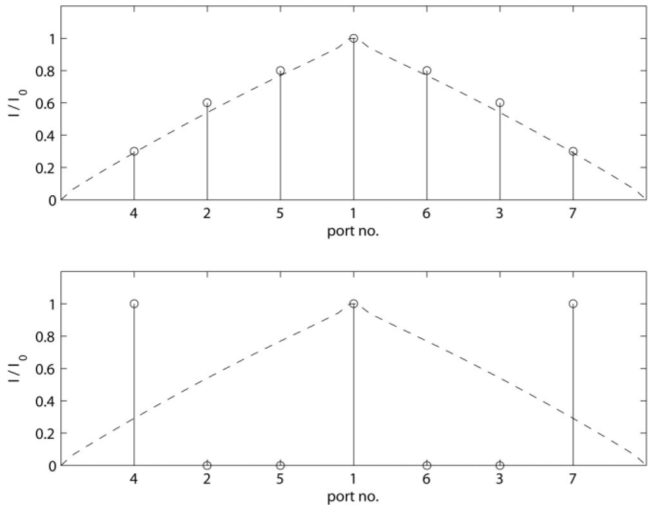

Figure 5 Excitation currents leading to minimum (top) and maximum (bottom) Q values corresponding to Figure 4. The dashed line marks the current distribution in the 1-port case

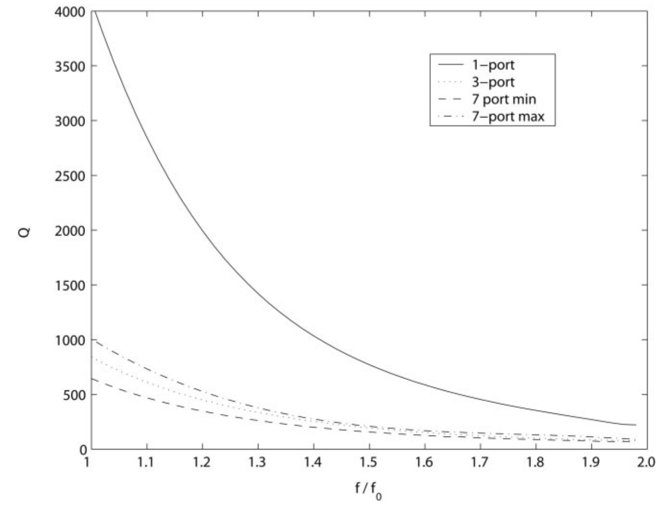

Figure 7 Q-values obtained with 1-port, 3-port, and 7-port loading

considered mirror symmetric, i.e., the same component values appear symmetrically on both sides of the wire. Now, by using the relationships of the Z-matrix of Section 2, the input impedance and Q of the antenna may be computed from the simulation data using (20). The loading is adjusted such that the antenna becomes resonant at f_0.

In Figure 7 the Q factors of the impedance loaded multiport antenna are shown. In the 1-port case the antenna is loaded with an inductor (whose reactance at $\omega_0 = 2\pi f_0$ is $\omega_0 L = 327\Omega$) at the feed point. In the 3-port case, the antenna is loaded with capacitors at ports 2 and 3, and in the 7-port case at ports 2–7. In the 7-port case, the capacitance values leading to minimum and maximum Q factors were sought with a Matlab routine when the reactances $1/\omega_0 C$ varied between 80 and 1600Ω. The reactances corresponding to the Q curves presented in Figure 7 are given in Table 1. As is seen in Figure 7, loading the antenna with an inductor at the feed port increases notably the Q factor of the antenna system compared to the unloaded 1-port element (see Figure 2). On the contrary, the capacitor loading in the 3-port case leads to remarkably smaller Qs, and with a certain 7-port capacitance loading yet smaller Q factors are possible.

4. CONCLUSIONS

In this article, we have derived an expression for the Q of a multiport antenna based on the total field energy stored by the antenna system. Some fundamental relationships derived from the basic electric network equations have also been presented that enable the design and control of the impedance properties of multiport antennas using the impedance (or admittance) matrix obtained, for instance, from electromagnetic simulations or real antenna measurements (by way of the relevant scattering matrix). The derived formulae were subsequently applied numerically in the search for optimal (in terms of smallest Q) loading and excitation of a multiport antenna. The example structure considered by means of HFSS simulations was an electrically short wire. The results confirm that a set of suitably chosen load impedances distributed within the antenna structure may indeed improve the Q as compared to the case where the antenna is conjugate matched at the feed point. It was also found that an appropriately chosen set of excitation currents may lead to a better Q than that obtained by feeding the antenna from a single point.

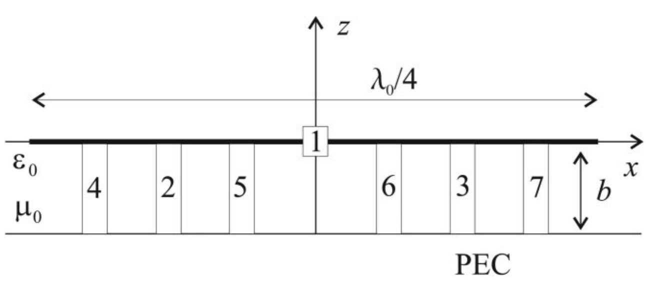

Figure 6 Horizontal dipole with multiple loading ports

APPENDIX

In a typical multiport antenna application scenario, where one of the ports is adopted as the input/output and the others are loaded with suitable impedances z_{Li}, we are required to find the impedance seen at the input. In this case, the antenna (modeled by the impedance matrix $\bar{\bar{Z}}$) is connected through its terminals to the diagonal load impedance matrix $\bar{\bar{Z}}_L$. Thus, combining (1) with $\bar{V} = -\bar{\bar{Z}}_L \bar{I}$ renders $(\bar{Z} + \bar{Z}_L)\,\bar{I} = 0$. To have an existing solution, apart from the trivial $\bar{I} = \bar{0}$, the determinant of this eigenvalue equation must vanish, i.e., [12] $\det(\bar{\bar{Z}} + \bar{Z}_L) = \bar{0}$, which leads to an equation that can be solved analytically in the case of a small number of ports and, more generally, numerically. Explicitly, we have

$$\begin{vmatrix} z_{11} + z_{L1} & z_{12} & \cdots & z_{1N} \\ z_{21} & \ddots & & z_{2N} \\ \vdots & & \ddots & \\ z_{N1} & \cdots & & z_{NN} + z_{LN} \end{vmatrix} = 0 \tag{21}$$

and, supposing that the port number 1 be the unknown element, we obtain

Table 1 Tuning Reactances

port no.	4	2	5	6	3	7
$1/\omega_0$C [Ω](3-port)	-	118	-	-	118	-
$1/\omega_0$C [Ω](7-port min)	200	1064	1590	1590	1064	200
$1/\omega_0$C [Ω](7-port mx)	1590	357	82	82	357	1590

$$z_{L1} = -z_{11} + \frac{1}{M_{11}} \sum_{j=2}^{N} (-1)^j z_{1j} M_{1j} \quad (22)$$

where M_{ij} is the minor (or secondary determinant, obtained by deleting row i and column j) of the matrix $\overline{\overline{Z}} + \overline{\overline{Z}}_L$. Requiring equality of the input impedance and the load impedance, and generalizing the result to the input impedance viewed at the kth port yields

$$Z_{\text{in},k} = z_{kk} + \frac{1}{M_{kk}} \sum_{j=1,\, j \neq k}^{N} z_{kj} C_{kj} \quad (23)$$

where $C_{kj} = (-1)^{j+k} M_{kj}$ is the cofactor of the corresponding minor M_{kj}. In particular, for the two port system ($N = 2$), we have the well-known result [3, 12]

$$Z_{\text{in}} = z_{11} - \frac{z_{12} z_{21}}{z_{22} + z_{2L}} \quad (24)$$

where $z_{12} = z_{21}$ if the network is reciprocal, as is usually the case.

REFERENCES

1. H. Steyskal and J.S. Herd, Mutual coupling compensation in small array antennas, IEEE Trans Antennas Propag 38 (1990), 1971–1975.
2. H.D. Foltz and J.S. McLean, Bandwidth limitations on antenna systems with multiple isolated input ports, Microwave Opt Technol Lett 19 (1998), 301–304.
3. R.F. Harrington, Field computation by moment methods, Chapter 6, MacMillan, New York, 1968.
4. F. Schwering, N.N. Puri, and C.M. Butler, Modified diakoptic theory of antennas, IEEE Trans Antennas Propag 34 (1986), 1273–1281.
5. R.L. Fante, Quality factor of general ideal antennas, IEEE Trans Antennas Propag 17 (1969), 151–155.
6. W. Geyi, P. Jarmuszewski, and Y. Qi, The Foster reactance theorem for antennas and radiation Q, IEEE Trans Antennas Propag 48 (2000), 401–408.
7. A.D. Yaghjian and S.R. Best, Impedance, bandwidth and Q of antennas, IEEE Trans Antennas Propag 53 (2005), 1298–1324.
8. L. Li and C.-H. Liang, Analysis of resonance and quality factor of antenna and scattering systems using complex frequency method combined with model-based parameter estimation, Prog Electromagn Res 46 (2004), 165–188.
9. C.H. Papas, Theory of electromagnetic wave propagation, Dover, New York, 1988.
10. A.D. Yaghjian, Improved formulas for the Q of antennas with highly lossy dispersive materials, Antennas Wireless Propag Lett 5 (2006), 365–369.
11. E.A. Marengo, A.J. Devaney, and F.K. Gruber, Inverse source problem with reactive power constraint, IEEE Trans Antennas Propag 52 (2004), 1586–1595.
12. N. Marcuwitz, Network formulation of electromagnetic field problems, Proceedings of the Symposium of Modern Network Synthesis, New York, Polytechnic Institute of Brooklyn, 1952, 215–235.

INVESTIGATION OF LOW-PROFILE FRESNEL ZONE PLATE ANTENNAS

S. M. Stout-Grandy,[1] A. Petosa,[2] I. V. Minin,[3] O. V. Minin,[3] and J. S. Wight[1]

[1] Department of Electronics, Carleton University, 1125 Colonel By Drive, Ottawa, Ontario, K1S 5B6 Canada; Corresponding author: sstout@doe.carleton.ca
[2] Advanced Antenna Technology Group, Communications Research Centre Canada, 3701 Carling Ave., Ottawa, K2H 8S2 Canada
[3] Department of Information Protection, Novosibirsk State Technical University (NSTU), 20 Karl Marx Prospect, Novosibirsk, 630092 Russia

Received 14 December 2007

ABSTRACT: *This article presents low-profile configurations of the Fresnel zone plate antenna at Ka-band. The investigation involved progressively reducing the focal distance of the antenna through simulations and observing the effect on the directivity, radiation patterns, and aperture efficiency. The number of metal zones was also varied in the simulations. It was found that focal distances below 0.75λ yielded little more directivity than the feed itself. With a single zone, the 1.25λ focal distance achieved the highest overall aperture efficiency of 24%, which was a significant improvement over the larger focal distance cases. Measurements were performed to verify the simulated results.* © 2008 Wiley Periodicals, Inc. Microwave Opt Technol Lett 50: 2039–2043, 2008; Published online in Wiley InterScience (www.interscience.wiley.com). DOI 10.1002/mop.23593

Key words: *Fresnel zone plate antenna; low-profile*

1. INTRODUCTION

The Fresnel zone plate antenna (FZPA) is a type of microwave lens, which originated from the work of Augustin Fresnel in the early 19th century at optical frequencies [1]. In its standard configuration, as shown in Figure 1, it is planar in the xy plane and has a feed antenna situated at the focal point of the lens at a distance F along the z-axis. The aperture of the FZPA consists of circular zones that alternate between transparent and metal, which focus the fields using the principle of diffraction [2].

FZPAs are very attractive for applications in the Ka-band where they offer significant advantages over shaped lenses, parabolic reflectors, and planar arrays. The FZPA is much simpler to fabricate, has a reduced aperture thickness, is lighter weight, and is an overall lower cost antenna solution. Despite these tremendous advantages, they have not been widely used in the past. This is primarily because of their low aperture efficiency, which is due to the blocking of a large percentage of EM waves by the metal

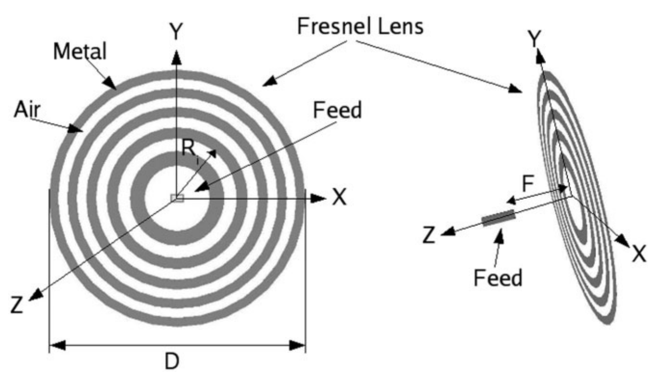

Figure 1 Fresnel zone plate antenna: (a) front view and (b) isometric view